

Investigating the synergistic potential Si and biochar to immobilize soil Ni in a contaminated calcareous soil after *Zea mays* L. cultivation

Hamid Reza Boostani¹, Ailsa G. Hardie², Mahdi Najafi-Ghiri¹, Ehsan Bijanzadeh³, Dariush Khalili⁴, Esmail Farrokhnejad¹

¹Department of Soil Science, College of agriculture and natural resources of Darab, Shiraz University, Darab74591, Iran.

²Department of Soil Science, Faculty of AgriSciences, Stellenbosch University, Private Bag X1, Matieland 7602, South Africa

³Department of agroecology, College of agriculture and natural resources of Darab, Shiraz University, Darab 74591, Iran

⁴Department of Chemistry, College of Sciences, Shiraz University, Shiraz 71454, Iran

Correspondence to: Hamid Reza Boostani (hr.boostani@shirazu.ac.ir)

Abstract. In Iran, a significant percentage of agricultural soils are contaminated with a range of potentially toxic elements (PTEs), including Ni, which need to be remediated to prevent their entry into the food chain. Silicon (Si) is a beneficial plant element that has been shown to mitigate the effects of PTEs on crops. Biochar is a soil amendment that sequesters soil carbon, and that can immobilize PTEs and enhance crop growth in soils. No previous studies have examined the potentially synergistic effect of Si and biochar on soil Ni chemical fractions and immobilization. Therefore, the aim of this study was to examine the interactive effects of Si and biochar, to reduce soil Ni bioavailability and its corresponding uptake in corn (*Zea Mays*) in a calcareous soil. A 90-day factorial greenhouse study with corn was conducted. Si application levels were applied at 0 (S₀), 250 (S₁) and 500 (S₂) mg Si kg⁻¹ soil and biochar treatments (3% wt.) including rice husk (RH) and sheep manure (SM) biochars produced at 300°C and 500°C (SM300, SM500, RH300 and RH500). At harvest, corn shoot Ni-concentrations, soil chemical Ni fractions and DPTA-release kinetics were determined. Simultaneous utilization of Si and SM biochars led to a synergistic reduction (15-36%) of soluble and exchangeable soil Ni fractions compared to application of Si (5-9%) and SM (5-7%) biochars separately. The application of the Si and biochars also decreased DPTA-extractable Ni and corn Ni shoot concentration (by up to 57%), with the combined application of SM500+S₂ being the most effective. These effects were attributed to the transformation of Ni from more bioavailable fractions to more stable iron oxide bound fractions, related to soil pH increase. The SM500 was likely the most effective biochar due to its higher alkalinity and lower acidic functional group content which enhanced Ni sorption reactions with Si. The study demonstrates the synergistic potential of Si and sheep manure biochar at immobilizing Ni in contaminated calcareous soils.

1 Introduction

One of the most important ways for potentially toxic elements (PTEs) to enter the human food chain is through the consumption of plants grown in soils contaminated with PTEs. Potentially toxic elements pollute soil environments as a result of mining, metal smelting, use of sewage sludge and domestic and industrial effluents in agriculture especially in developing countries (Liu et al., 2018). Potentially toxic elements in soils cannot undergo biodegradation by

43 living organisms, so they possess great stability and longevity in the soil (Poznanović Spahić et
44 al., 2019). Unlike other PTEs found in soils, such as mercury (Hg), cadmium (Cd) and lead (Pb),
45 nickel (Ni) is essential for plant growth at very low concentrations. Nevertheless, at elevated
46 contents ($>35 \text{ mg Ni kg}^{-1}$ soil), Ni causes many physiological and morphological malfunctions in
47 plants and severely stunts their growth (Shahzad et al., 2018; Antoniadis et al., 2017). In a study
48 conducted by Shahbazi et al. (2022), the Ni weighted average concentration of the cultivated lands
49 of Iran in the vicinity of the industrial areas was reported 350 mg kg^{-1} soil. In these soils, the
50 pollution index (the ratio of the element concentration to the standard concentration) calculated
51 for the Ni is greater than 5, which indicates a severe degree of pollution from the point of view of
52 environmental protection. Shahbazi et al. (2020) collected 711 agricultural soil samples located at
53 different climate zones (extra arid, arid, semi-arid, Mediterranean, semi humid, humid and per-
54 humid based on the de Martonne classification system) of Iran and reported that the Ni content in
55 the soils was between 2.79 mg kg^{-1} and 770 mg kg^{-1} with an average of 68 mg kg^{-1} soil. The results
56 showed that the concentration of Ni in 11.3% of these soils was higher than the threshold value.
57 Removing PTEs from contaminated sites via traditional methods such as pump and treat
58 technologies, soil washing and excavation is very expensive and time-consuming, therefore, for
59 plant cultivation in these areas, low-cost and effective methods should be sought to stabilize PTEs
60 in soils and prevent them from being transferred to the plant (Gao et al., 2023).

61 Silicon (Si) is a valuable nutrient for plant growth, and it is only considered essential for
62 some plant species such as rice. Applying Si to the soil can enhance plant resistance against
63 biological and non-biological tensions, including physiological stress caused by PTEs in soil (Bhat
64 et al., 2019; Yan et al., 2018). The use of Si to promote plant growth and mitigate the toxicity of
65 PTEs is becoming increasingly popular in agriculture (Li, 2019; Adrees et al., 2015). The
66 application of Si in soils contaminated with PTEs may reduce the bioavailability of PTEs by
67 increasing soil pH, increasing the secretion of organic ligands by the roots and the formation of
68 insoluble compounds with PTEs, and ultimately enhancing plant growth (Bhat et al., 2019; Xiao
69 et al., 2021). The soil pH increase associated with Si application is attributed to the hydrolysis
70 reaction of the silicate anion in soil solution which generates hydroxyl ions (Ma et al. 2021).

71 Biochar is an organic soil amendment that sequesters soil carbon (C) that has received
72 much attention in recent years to stabilize PTEs in polluted sites (El-Naggar et al., 2018). Biochar
73 is a carbon-rich, porous organic material which is prepared in a limited or no oxygen conditions
74 by pyrolysis of organic wastes, including crop and animal residues, urban waste, wood byproduct
75 (Vickers, 2017; Ankita Rao et al., 2023). The organic surface functional groups of biochar such as
76 carboxylic and phenolic groups provide cation exchange capacity in soils (Tomczyk et al., 2020).
77 Addition of biochar to the soil not only improves the soil chemical and physical properties, but
78 also reduces the bioavailability of PTEs in contaminated soils through some physicochemical
79 processes such as sedimentation, complexation, and electrostatic adsorption (Bandara et al., 2020;
80 Deng et al., 2019; Derakhshan Nejad et al., 2018). The complexation of Ni with oxygen-containing
81 functional groups on biochar surfaces including carboxyl, ether, carbonyl, and hydroxyl, has been
82 identified as a key mechanism for Ni immobilization in soil (Alam et al., 2018; El-Naggar et al.,
83 2018). Electrostatic attraction of Ni by negatively charged functional groups on the surfaces of
84 biochar is another potential mechanism for soil Ni stabilization (Ahmad et al., 2014). Increased
85 soil pH following the application of biochar also promotes Ni adsorption reactions (Uchimiya et
86 al., 2010). However, the efficiency of biochar prepared from different feedstocks and under
87 different production conditions in stabilizing PTEs in soils can vary significantly (Dey et al., 2023).

88 Potentially toxic elements in soil can exist in different chemical fractions such as water
89 soluble and exchangeable (WsEx), bound to carbonates (CAR), organic matter (OM), iron and
90 manganese oxides (FeMnOx) and residual (Res) (found in minerals) (Singh et al., 1988). The
91 bioavailability of these forms differs, the WsEx fraction has the highest bioavailability and the Res
92 form is considered unusable by plants. PTEs in other chemical fractions in soils could be
93 potentially accessible for plant roots depending on soil characteristics such as soil texture, soil pH
94 and soil organic matter content (Kamali et al., 2011; Bharti et al., 2018). The diethylene triamine
95 penta-acetic acid (DTPA) extraction is commonly employed for assessing Ni availability in
96 calcareous soils (Lindsay and Norvell, 1978). However, it is important to acknowledge that this
97 methodology solely assesses Ni availability for plants, while the quantity of released Ni may vary
98 across distinct stages of plant development. Consequently, the examination of alterations in
99 extractable Ni levels over time using the DTPA solution can prove valuable in estimating soil Ni
100 bioavailability. The PTEs desorption capacities of soils are anticipated to be contingent upon
101 factors such as soil pH, cation exchange capacity, the specific nature of metal ions, and the source
102 of the metals (Kandpal et al., 2005). Furthermore, the release kinetic parameters can provide
103 insight into the bonding mechanisms of PTEs in soils and their potential risk for leaching into
104 groundwater or surface water (El-Naggar et al., 2021). Therefore, sequential extraction methods
105 and release kinetics models have been employed to assess the efficacy of amendment materials in
106 stabilizing PTEs in contaminated soils. Xiao et al. (2021) found that addition of mineral Si fertilizer
107 to a contaminated paddy soil caused a significant decrease in the Cd and Pb fractions bound to
108 carbonates and iron-manganese oxides while the residual and organic matter-bound forms
109 experienced a notable enhancement. In another study, application of cotton residue biochar (1.5
110 wt. %) to a calcareous soil with a sandy loam textural class containing different levels of Cd
111 contamination was more efficacious than corn and wheat straw biochars in decreasing the WsEx-
112 Cd and Car-Cd forms and enhancing the Res-Cd form. In addition, application of cotton residue
113 biochar decreased EDTA-extractable Cd by 45–52% compared to the control (Boostani et al.,
114 2023a).

115 As both biochars and Si are economical and effective soil amendments to reduce plant
116 uptake of PTEs and stress in contaminated soils, their potential synergistic effect on the
117 immobilization of PTEs in soils should be further investigated. Currently, no previous studies have
118 examined the combined application effects of Si and biochars on the chemical fractions and release
119 kinetics of Ni in calcareous soils. The primary objective of the present study was to elucidate the
120 interaction of biochars and Si levels, to reduce soil Ni bioavailability and its corresponding
121 accumulation in corn (*Zea Mays* L. 604) plant. Additionally, the study sought to elucidate the
122 underlying soil chemical mechanisms that are likely to be responsible for such effects.

123 2 Materials and methods

124 2.1 Soil sampling, characterization and Ni treatment

125 A composite soil sample from the surface layer (0-30 cm) was collected with an auger at
126 the research farm of the College of Agriculture and Natural Resources in Darab, southern Iran (28
127 ° 45' 0.99" N 54° 26' 52.14" E, Elevation 1105 m) (Fig. 1). The climate, mean annual
128 precipitation, soil moisture and thermal regimes of the studied area were semi-arid, 250 mm, ustic
129 and hyperthermic respectively. The soil sample was air-dried, passed through a 2 mm mesh, and
130 then physicochemical properties were determined. Soil sand, silt and clay content were determined
131 by sieving and the hydrometer method (Gee and Bauder, 1986). Soil pH and EC were determined
132 using a saturated paste (Rhoades, 1996), while organic matter was determined using Walkley-

133 Black procedure (Nelson and Sommers, 1996). Calcium carbonate equivalent (CCE) was
134 determined by acid neutralization (Loeppert and Suarez, 1996), while cation exchange capacity
135 was determined using 1M ammonium acetate (Merck, 99%) method (Sumner and Miller, 1996).
136 Available Ni was determined using DPTA (Merck, 99%) extraction (Lindsay and Norvell, 1978).
137 Plastic containers were filled with two kilograms of soil and then 500 ml NiCl₂ (Merck, 99%)
138 solution was mixed into to them to achieve a Ni concentration of 300 mg Ni kg⁻¹ soil. The Ni-
139 treated soil samples were then allowed to dry out at room temperature, and then rewetted to field
140 capacity using deionized water and allowed to dry out again. The rewetting and room temperature
141 drying cycle was repeated three times to allow the Ni to equilibrate with the soil (The incubation
142 period was 60 days and the ambient temperature was 25±2 °C)((Boostani et al., 2023c).

143



144

145 **Fig. 1. The location of soil sampling in Darab region, southern Iran.**

146

147 2.2 Production of biochar and its properties

148 The sheep manure and rice husk were respectively procured from an active animal
149 husbandry and rice mill factory situated in the Darab region, Fars province, Iran. Subsequently,
150 the raw materials underwent a 1-week period of air-drying, followed by electrical milling and
151 sieving through a 2 mm mesh. A slow pyrolysis procedure (2 h at 300 °C and 500 °C) in an oxygen-
152 limited environment was carried out to generate biochars from feedstocks (Anand et al., 2023).
153 The generated biochars were then cooled at ambient temperature and sieved with a 0.5 mm mesh
154 to ensure consistent particle size. The chemical characteristics of the biochars were assessed using
155 the following standard methods. Biochar pH and EC were determined in a 1:10 deionized water
156 suspension (Sun et al., 2014), while CEC was determined using the method of Abdelhafez et al.
157 (2014). Biochar total C, N and H contents were determined by elemental analyzer
158 (ThermoFinnigan Flash EA 1112 Series, ThermoFinnigan, USA). Biochar moisture and ash
159 content were determined by heating in an oven, while the O+S content was calculated by
160 subtraction of C, N, H, ash and moisture content from total biochar mass (Keiluweit et al., 2010).
161 Biochar total Ni content was determined by combustion and dissolution of the ash in 2M HCl

162 (Merck, 37%) (Boostani et al., 2018a). The Ni content in the acid solution was determined using
 163 atomic absorption spectroscopy (AAS) (PG 990, PG Instruments Ltd., UK). The biochar surface
 164 functional groups were assessed using Fourier Transform Infrared (FTIR) spectroscopy using a
 165 Shimadzu DR-8001 instrument and KBr pellet transmission method. Biochar morphology was
 166 assessed using scanning electron microscopy (SEM) (TESCAN-Vega3, Czech Republic).

167 2.3 Greenhouse experiment

168 A completely randomized factorial experiment was conducted in a greenhouse
 169 environment with three replications. The first factor consisted of the biochar treatments including
 170 rice husk (RH) and sheep manure (SM) generated at 300 °C and 500 °C (Control (C) (with no
 171 biochar), SM300, SM500, RH300 and RH500), each at the level of 3%wt. The second factor
 172 included Si application levels (0 (S₀), 250 (S₁) and 500 (S₂) mg Si kg⁻¹ soil) supplied as Na₂SiO₃
 173 (Sigma Aldrich, 98%) solution. Based on the experimental design, Si levels were added to the 2
 174 kg of Ni-treated soil samples and after drying the soil and mixing it, the prepared biochars were
 175 added to the required amount. Immediately after that, the treated soil samples were transferred to
 176 plastic pots (45 pieces each containing 2 kg soil) and to facilitate the required reactions, the
 177 moisture content of the samples was kept at field capacity level for a duration of two weeks.
 178 Thereafter, 6 corn seeds (*Zea mays* L. 604) were planted in each pot, and at the 4-leaf stage, 2
 179 plants were kept in each pot until the end of cultivation. During the growth of the plant, distilled
 180 water was used to maintain the soil moisture content in the pots at field capacity. After 90 days,
 181 the plants were harvested at the soil interface, rinsed with distilled water to remove contamination,
 182 immediately air-dried and kept for Ni determination of plant shoots. After separating the roots
 183 and air drying, the soil from the pots was sifted via a 2 mm mesh, and subsequently utilized for
 184 performing Ni release kinetics experiment and determining the Ni chemical fractions.

185 2.4 Sequential extraction procedure

186 The present study employed a successive extraction technique (Singh et al., 1988) to
 187 fractionate soil nickel (Ni) in the following chemical forms, namely water-soluble and
 188 exchangeable (WsEx), carbonate-bound (Car), organic matter-bound (OM), manganese oxide-
 189 bound (MnOx), amorphous iron oxide-bound (AFeOx), crystalline iron oxide-bound (CFeOx), and
 190 residual (Res). The methodological specifics are provided in Table 1.

Table 1
 Successive extraction technique of Singh et al. (1988)

Chemical speciation containing Ni	acronym	Duration of agitation (h)	Extractants	Relative density (g.cm ⁻³)
Exchangeable and soluble	WsEx	2	1 M magnesium nitrate (Merck, 98%)	1.10
Carbonate	Car	5	1 M sodium acetate (Merck, 99%) (pH=5)	1.04
Organic	OM	0.5	0.7 M sodium hypochloride (pH=8.5)	1.00
Mn oxide	MnOx	0.5	0.1 M hydroxyl amine hydrochloride (Merck, 98%) (pH=2 by nitric acid (Merck, 65%))	1.00
Amorphous Fe oxides	AFeOx	0.5	0.25 M hydroxyl amine hydrochloride (Merck, 98%) + 0.25 M chloridric acid (Merck, 37%)	1.01
Crystalline Fe oxides	CFeOx	0.5	0.2 M ammonium oxalate (Merck, 99%) + 0.2 M oxalic acid (Merck, 99%) + 0.1 M ascorbic acid (Merck, 99.7%)	1.02

191 2.5 Release kinetics experiment

192 A fifty-milliliter centrifuge tube was filled with 10 g of soil. After that, 20 ml of DTPA
193 solution (0.005 M DTPA (Merck, 99%) + 0.1 M tri-ethanol amine (Merck, 99%) + 0.01 M calcium
194 chloride (Merck, 97%)) (pH: 7.3) (Lindsay and Norvell, 1978) was added to the soil. The soil-
195 DTPA mixtures were stirred for specific periods of time, i.e. 5, 15, 30, 60, 120, 360, 720 and 1440
196 minutes at a constant temperature (25 ± 2 °C). After each stirring time, the soil suspension was
197 centrifuged ($2683 \times g$) to separate the soil particles from the liquid phase. Atomic absorption
198 spectroscopy (AAS) (PG 990, PG Instruments Ltd., UK) was used to analyze the Ni concentration
199 in the liquid phase. The Ni concentration in the liquid phase versus time was plotted to obtain a Ni
200 release kinetic curve. A total of seven kinetic models namely order models (zero, first, second and
201 third), parabolic diffusion, power function and simple Elovich were assessed to fit the Ni release
202 data. The best models for describing the data were selected according to the maximum value of
203 the coefficient of determination (R^2) and the minimum amount of the standard error of estimate
204 (SEE) (Nasrabadi et al., 2022).

205 2.6 Data analysis

206 The ANOVA test was utilized to assess treatments effects between the individual and
207 combined biochar and silicon treatments. Additionally, a comparison of means was conducted
208 using the MSTATC computer program, applying Duncan's test with a significance level of 5%.
209 Figures were generated using Excel 2013 software. Pearson correlation coefficients among
210 parameters in the dataset were determined using SPSS 12.0.

211 3 Results and Discussion

212 3.1 Soil characteristics

213 The soil used in the study prior to experimental treatment, exhibited a sandy loam texture
214 and possessed alkaline properties with significant calcium carbonate content, while not being
215 classified as saline (Table 2). The quantity of soil organic matter was extremely low, a distinct
216 characteristic of soils from arid and semi-arid regions (Okolo et al., 2023) (Table 2). The relatively
217 low levels of clay and organic matter present in the soil contributed to a correspondingly low soil
218 cation exchange capacity (CEC) (Table 2). The soils in Iran mainly originate from calcareous
219 alluvium under xeric, ustic or aridic and mesic, thermic or hyperthermic moisture and temperature
220 regimes, respectively. These soils have varied properties such as calcium carbonate equivalent (1-
221 81%), clay content (1-75%), EC (0.4-49.0 dS m^{-1}), organic matter (0.1-21.5%) and gypsum content
222 (0-91%) (Ghiri et al., 2011). Furthermore, it should be noted that the concentration of available
223 soil Ni extractable by DTPA was very low (Table 2).

224

225

226

227

228

Table 2
Certain physicochemical attributes of the soil prior to cultivation.

Sand (%)	58.0
Silt (%)	30.0
Clay (%)	12.0
Soil textural class	Sandy loam
pH _(s)	7.59
EC (dS m ⁻¹)	2.60
CCE (%)	55.0
OM (%)	0.50
CEC (cmol ₍₊₎ kg ⁻¹)	11.7
Total Ni (mg kg ⁻¹)	28.0
Ni-DTPA (mg kg ⁻¹)	0.39

Notes: EC, electrical conductivity; OM, organic matter; CCE, calcium carbonate equivalent; CEC, cation exchange capacity.

229

230 3.2 Chemical characteristics of the biochars

231 As the pyrolysis temperature rose from 300 °C to 500 °C, the SM biochars demonstrated
232 elevated pH and EC values, with the highest levels observed at the highest temperature (Table 3).
233 The elevated levels of alkali salts, which are reflected in the high ash content (Table 3), are the
234 contributing factor behind this observation in the SM biochars in comparison to the RH biochars.
235 Plant-based biochars commonly exhibit reduced levels of dissolved solids in comparison to
236 animal-based biochars (Sun et al., 2014). The SM300 biochar possessed the highest CEC value of
237 19.70 cmol₍₊₎ kg⁻¹. The observed phenomenon may be attributed to the diminution of surface
238 functional groups, namely carboxyl and phenol, at elevated pyrolysis temperatures. These groups
239 are predominantly responsible for facilitating the cation exchange capacity (CEC) of biochars
240 (Tomczyk et al., 2020). As the pyrolysis temperature increased, there was an observed increase in
241 the C content of the biochars, and a corresponding decrease in the content of hydrogen, oxygen,
242 and nitrogen (Table 3). The observed increase in the concentration of C as pyrolysis temperature
243 rises is consistent with a concomitant rise in the degree of carbonization. The observed reduction
244 in the levels of H and O might be attributed to the occurrence of dehydration reactions,
245 decomposition of oxygenated bonds, and the liberation of low molecular weight byproducts rich
246 in H and O, as recently noted by Zhao et al. (2017). Nitrogen compound volatilization explains the
247 diminished N content of the biochars at elevated pyrolysis temperatures. The ratios of H:C and
248 O:C are significant indicators of the aromaticity and polarity of biochars; the lower the ratios the
249 more condensed aromatic C the biochar contains (Chatterjee et al., 2020). The results shown in
250 Table 3 indicate that the H:C and O:C mole ratios showed a gradual decrease as the pyrolysis
251 temperature was increased, which can be interpreted as a sign of improved carbonization of the
252 biochars (Zhao et al., 2017). The Ni content in the biochars derived from rice husk was below
253 detection, whereas a limited quantity of Ni was detected in the biochars produced from sheep
254 manure (Table 3).

255

256

Table 3
Some physical and chemical properties of the biochars.

	SM300	SM500	RH300	RH500
pH (1:20)	9.96	11.0	9.0	10.3
EC (1:20) (dS m ⁻¹)	3.94	4.28	0.84	1.17
CEC (cmol _c kg ⁻¹)	19.7	18.9	18.9	15.3
C (%)	25.4	31.8	45.0	50.0
H (%)	1.85	0.8	2.28	1.06
N (%)	2.10	1.57	1.30	1.10
Ni (mg kg ⁻¹)	3.0	15.4	Nd	Nd
Moisture content (%)	1.91	1.82	2.65	2.37
Ash content (%)	53.8	60.0	34.2	44.8
H:C mole ratio	0.87	0.30	0.60	0.25
O+S:C mole ratio	0.44	0.09	0.24	0.01

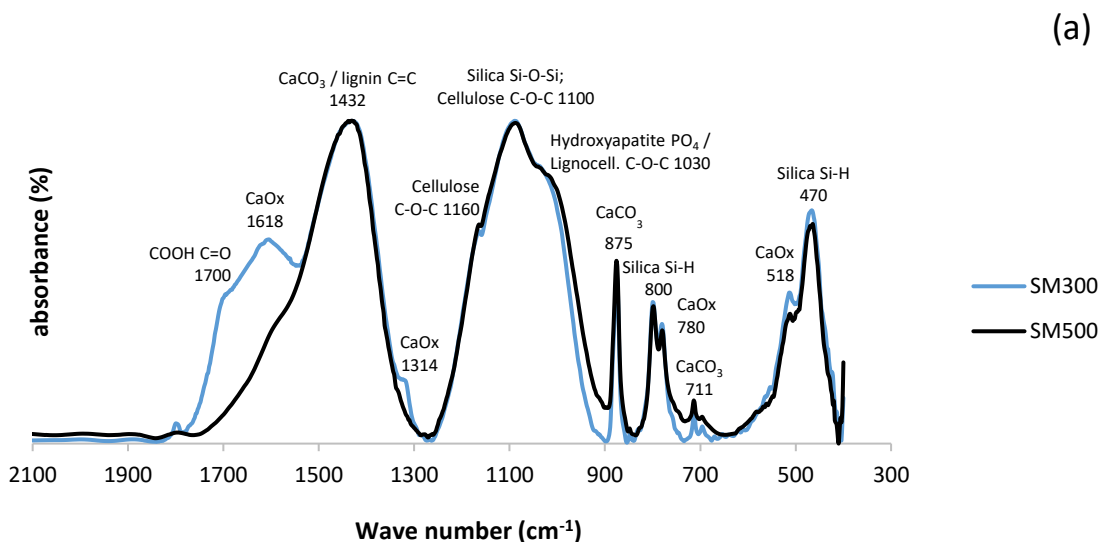
Notes: SM300, sheep manure biochar generated at 300 °C; SM500, sheep manure biochar generated at 500 °C; RH300, rice husk biochar produced at 300 °C; RH500, rice husk biochar produced at 500 °C; CEC, cation exchange capacity; EC, electrical conductivity; Nd, non-detectable.

257

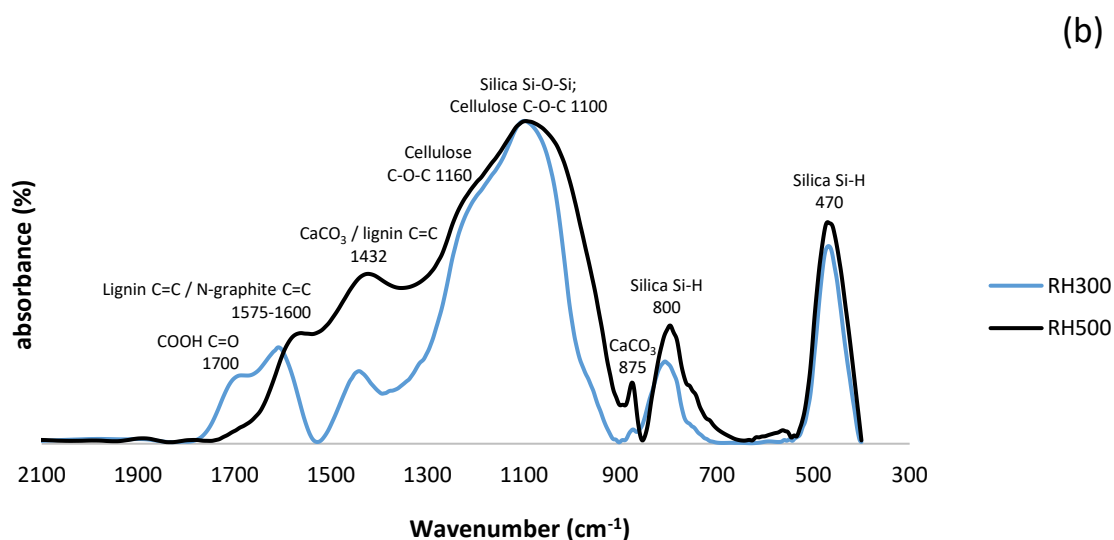
258 3.3 Biochar analysis using FTIR and SEM

259 The FTIR spectra of the SM and RH biochars are shown in Figure 2. The SM and RH
 260 biochars produced at 300 °C contained a higher content of carboxyl groups (1700 cm⁻¹) (Keiluweit
 261 et al., 2010) than the biochars produced at 500 °C, which is in agreement with the O:C values of
 262 the biochars (Table 3). All of the biochars contained absorption bands associated with lignin (1430
 263 cm⁻¹) and cellulose (1030 -1160 cm⁻¹) (Keiluweit et al., 2010). The SM biochar contained more
 264 calcite than the RH biochar as indicated by the greater intensity of calcite characteristic peaks at
 265 1432, 875, and 711cm⁻¹ (Myszka et al., 2019) in the SM biochars (Fig. 2a). There was also
 266 evidence of the presence of Ca oxalate in the SM biochars, indicated by the characteristic peaks at
 267 1618, 780 and 518 cm⁻¹ (Maruyama et al., 2023). All the biochars contained silica as indicated by
 268 the intense silica absorption peaks at 1100, 800 and 470 cm⁻¹ (Zemnukhova et al., 2015).

269



270

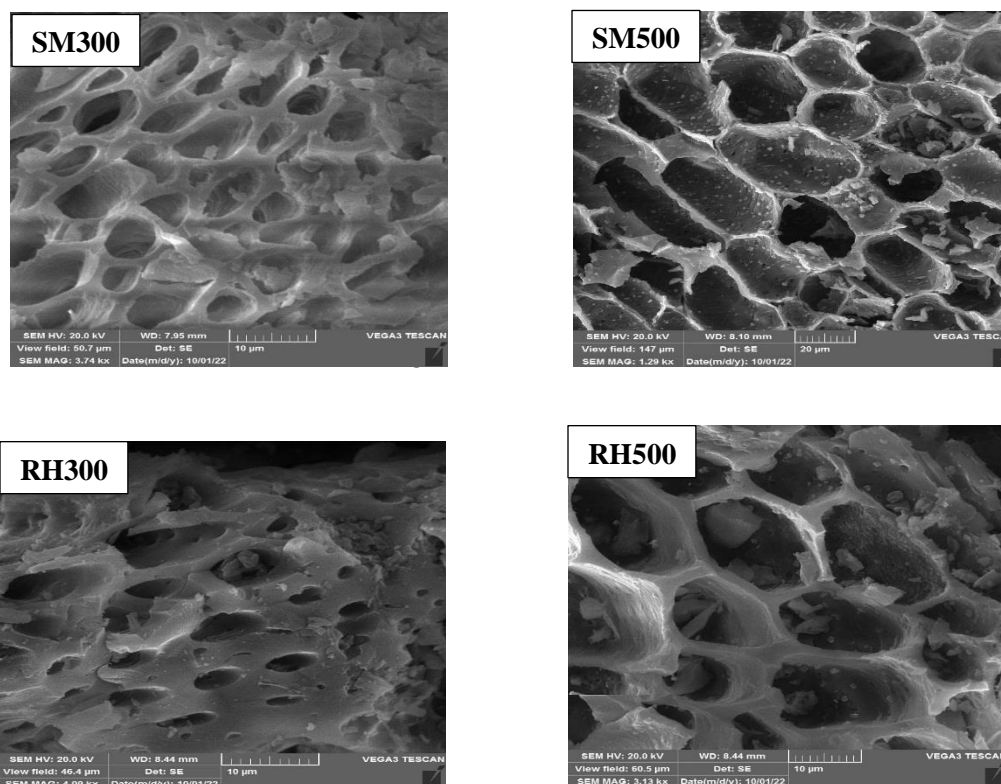


271

272 **Fig. 2.** FTIR spectra the biochars in the wave number range of 400-2000 cm^{-1} . Notes: SM300, sheep
 273 manure biochar produced at 300 °C; SM500, sheep manure biochar produced at 500 °C; RH300, rice husk biochar
 274 produced at 300 °C; RH500, rice husk biochar produced at 500 °C.

275

276 The SEM images of the SM and RH biochars are shown in Figure 3. The morphology of
 277 the biochars became more rigid and porous at higher temperatures, as evidenced by the cell wall
 278 shrinkage attributed to devolatilization of organic tissues (Claoston et al., 2014).



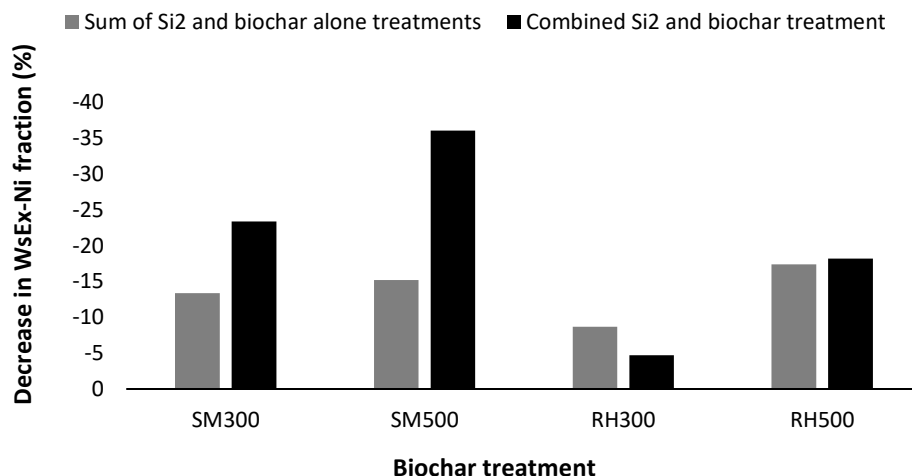
280

281 **Fig. 3.** SEM images of the biochars. Notes: SM300, sheep manure biochar produced at 300 °C; SM500, sheep
 282 manure biochar produced at 500 °C; RH300, rice husk biochar produced at 300 °C; RH500, rice husk biochar produced
 283 at 500 °C.
 284

285 3.4 Soil Ni chemical fractions after the application of Si levels and biochars

286 The interaction of treatments (biochars and Si levels) had a statistically significant effect
 287 ($P < 0.01$) on all the soil Ni chemical fractions, except for the Ni-Car fraction, while the main effects
 288 on all the soil Ni chemical forms were significant. The soil Ni concentration in the WsEx fraction
 289 was significantly reduced by the application of Si levels (S_0 to S_2) from $6.07 \text{ mg Ni kg}^{-1}$ to 5.17
 290 mg Ni kg^{-1} by 14.8% (Table 4). Among the biochar treatments, the greatest decrease in WsEx-Ni
 291 fraction compared to the control was due to SM500 from $6.04 \text{ mg Ni kg}^{-1}$ to $5.01 \text{ mg Ni kg}^{-1}$ by
 292 17%, while the RH300 treatment had no significant effect (Table 4). The interaction effect of
 293 treatments indicated that the lowest WsEx-Ni concentration was due to the combined treatment of
 294 SM500+ S_2 ($4.04 \text{ mg Ni kg}^{-1}$ soil) (Table 4). The combined treatment of S_2 and SM biochars had
 295 strong synergistic effect on reducing WsEx-Ni fraction (23-36% reduction) compared to the sum
 296 of the treatments alone (13-15% reduction) (Fig. 4). Whereas this synergistic effect of the
 297 combined treatments was not evident for the RH biochars (Fig. 4). There was a negative correlation
 298 between soil Ni-WsEx fraction and soil pH ($r = -0.66, p < 0.01$) indicating that the reduction in
 299 Ni-WsEx fraction was strongly linked to the increase in soil pH due to the amendments. Previous
 300 studies have also shown that application of biochars and silicates result in increases in soil pH,
 301 thus reducing the bioavailability of PTEs and their conveyance to plant roots (Shen et al., 2020;
 302 Ma et al., 2021). Among the applied biochars, the maximum pH and ash content (Table 3) and
 303 calcite (lime) content (Fig. 2) were attributed to the SM500 biochar. Therefore, the combined

304 SM500+S₂ was most effective at reducing WsEx-Ni fraction, likely due to the higher alkalinity
305 and ash content of SM500 promoting Ni precipitation and adsorption (Sachdeva et al., 2023).



306
307 **Fig. 4.** Comparison of the effect of sum of the Si₂ and biochar alone treatment versus the combined
308 Si₂ and biochar treatments on the % reduction of the WsEx-Ni fraction. Notes: SM300, sheep manure
309 biochar produced at 300 °C; SM500, sheep manure biochar produced at 500 °C; RH300, rice husk biochar produced
310 at 300 °C; RH500, rice husk biochar produced at 500 °C.

311 The reduced effectiveness of biochars produced at 300 °C, as compared to those produced
312 at 500 °C, in decreasing soil Ni-WsEx content **could be** attributed to the lower rates of microbial
313 oxidation and mineralization of RH500 and SM500, which is **reflected in** their **greater**
314 environmental stability (as **indicated** by **the** lower H/C mole ratio values) (Table 3). Consequently,
315 biochar produced at 500 °C may not provide sufficient acidic carboxyl functional groups to the
316 soil to stimulate SOM decomposition, leading to a greater increase in soil pH (Sun et al., 2023).
317 According to Zhu et al. (2015), the addition of wine lees-based biochar (a material from a wine
318 processing factory) to a heavy metal-contaminated soil (at **levels** of 0.5% and 1% w/w) resulted in
319 an increase in soil pH and a decrease in the soil Ni content in the WsEx fraction. Furthermore, the
320 increase in soil pH due to the increase in Si levels may lead to the precipitation of Ni in the forms
321 of Ni silicate and hydroxide. Due to the high solubility of Na metasilicate, the hydrolysis of silicate
322 anion in the soil solution is intensified, leading to a high concentration of OH⁻ and a subsequent
323 increase in soil pH (Ma et al., 2021).

324
325
326
327
328
329
330

Table 4Effects of biochars and Si application levels on the soil Ni chemical fractions (mg kg⁻¹) after corn cultivation.

	C	SM300	SM500	RH300	RH500	Mean
	WsEx					
S ₀	6.32 a	6.02 a-c	5.91 bc	6.31 a	5.77 c	6.07 A
S ₁	6.03 a-c	5.37 d	5.09 de	6.25 ab	5.28 d	5.60 B
S ₂	5.77 c	4.84 e	4.04 f	6.02 a-c	5.17 de	5.17 C
Mean	6.04 A	5.41 B	5.01 C	6.20 A	5.41 B	
	OM					
S ₀	9.72 a	10.15 a	8.04 d-f	10.08 a	9.02 b	9.40 A
S ₁	9.60 a	9.75 a	7.16 g	8.62 b-d	8.70 bc	8.76 B
S ₂	8.11 c-f	7.94 ef	7.12 g	8.30 c-e	7.63 fg	7.82 C
Mean	9.14 A	9.28 A	7.44 C	8.99 A	8.44 B	
	MnOx					
S ₀	11.58 a	3.77 kl	5.99 f	4.69gh	9.71 c	7.15 A
S ₁	10.33 b	3.50 l	5.00 g	4.57 hi	8.93 d	6.48 B
S ₂	10.28 b	2.98 m	4.28 ij	3.96 jk	7.94 e	5.89 C
Mean	10.73 A	3.42 E	5.09 C	4.41 D	8.86 B	
	AFeOx					
S ₀	11.1 ef	10.4 g	11.8 d	11.0 fg	11.7 de	11.2 C
S ₁	12.2 b-d	10.7 fg	12.0 cd	12.2 b-d	12.7 bc	12.0 B
S ₂	12.8 b	12.2 b-d	12.2 b-d	12.3 b-d	14.2 a	12.7 A
Mean	12.1 B	11.1 C	12.0 B	11.8 B	12.9 A	
	CFeOx					
S ₀	77.3 f	78.00 f	84.0 cd	84.7 cd	79.6 ef	80.7 C
S ₁	77.9 f	82.2 de	86.3 bc	85.1 b-d	83.6 cd	83.0 B
S ₂	79.9 ef	85.5 bc	87.9 ab	85.7 bc	90.4 a	85.9 A
Mean	78.4 C	81.9 B	86.0 A	85.2 A	84.5 A	
	Res					
S ₀	200 c-e	207 a	200 c-e	196 f	198 d-f	200 A
S ₁	200 c-e	204 b	200 c-e	197 ef	195 f	199 A
S ₂	200 cd	204 b	201 c	199 c-e	190 g	199 A
Mean	200 B	205 A	200 B	198 B	195 BC	

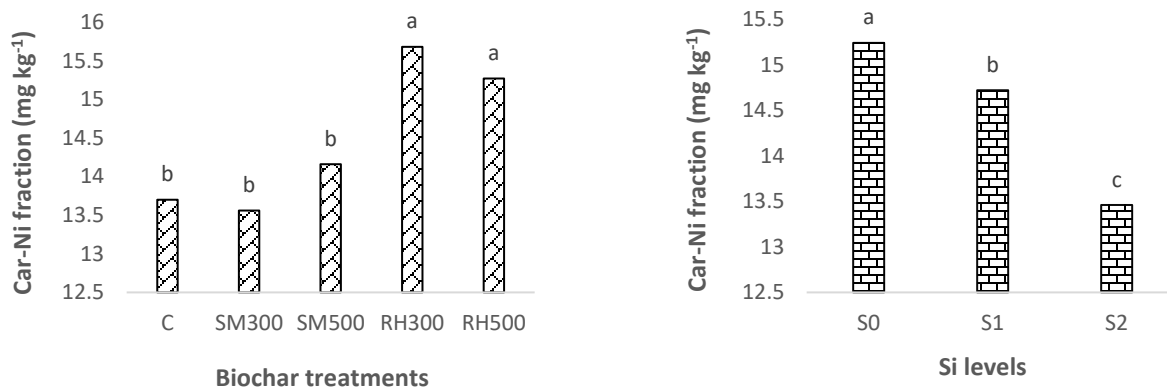
Notes: C, control; SM300, sheep manure biochar produced at 300 °C; SM500, sheep manure biochar produced at 500 °C; RH300, rice husk biochar produced at 300 °C; RH500, rice husk biochar produced at 500 °C; S₀, without Si addition; S₁, application of 250 mg Si kg⁻¹ soil; S₂, application of 500 mg Si kg⁻¹ soil. WsEx, water soluble and exchangeable fraction; OM, organic fraction; MnOx, bound to manganese oxides; AFeOx, bound to amorphous iron oxides; CFeOx, bound to crystalline iron oxides; Res, residual fraction; MF, mobility factor.

*Numbers followed by same letters in each column and rows, in each section, are not significantly (P<0.05) different

331 Si application levels from S₀ to S₂ significantly decreased the soil Ni content in the Car
 332 fraction by 11.7% (from 15.2 mg Ni kg⁻¹ soil to 13.5 mg Ni kg⁻¹ soil) (Fig. 5). The decrease in the
 333 concentration of Ni in the carbonate form with an increase in the Si levels could potentially be
 334 explained by the competition between silicate (SiO₄⁴⁻) and carbonate ions for binding with Ni²⁺
 335 ions in the soil solution (Sparks et al., 2022). The SM biochars had no significant effect on the
 336 Car-Ni fraction whereas addition of RH biochars led to a significant increase in this fraction (Fig.
 337 4). Ippolito et al. (2017) found that addition of two biochars (pine [*Pinus contorta*] and tamarisk
 338 [*Tamarix* spp.]) to a soil contaminated by mining activities caused a significant increase in the soil
 339 Cd content bound to carbonates. They concluded that the reduction in Cd bioavailability may have
 340 been due to the ability of biochar to raise soil pH levels and induce the precipitation of CdCO₃.
 341 Similarly, Yuan et al. (2011) proposed that the decrease in bioavailability of PTEs in soil amended
 342 by biochars derived from different crop residues might have been caused by the creation of metal-

343 carbonate species and carbonate-surface functional group reactions, which could function as a
344 mechanism for sequestration.

345



346

347 **Fig. 5.** Effects of (a) biochars and (b) **Si application levels** on the soil Ni concentration (mg kg⁻¹)
348 in the carbonate-bound fraction after corn cultivation. Notes: C, control; SM300, sheep manure biochar
349 produced at 300 °C; SM500, sheep manure biochar produced at 500 °C; RH300, rice husk biochar produced at 300 °C;
350 RH500, rice husk biochar produced at 500 °C; S₀, without Si addition; S₁, application of 250 mg Si kg⁻¹ soil; S₂,
351 application of 500 mg Si kg⁻¹ soil. * Numbers followed by same letters in each section, are not significantly (P<0.05)
352 different.

353

354 The biochars produced at 300 °C had no significant effect on the OM-Ni fraction compared
355 to control, while the biochars generated at 500 °C significantly decreased it (Table 4). **the greatest**
356 **reduction in soil Ni content in the OM fraction (18.6%) was found to be in that which underwent**
357 **the SM500 treatment.** Lu et al. (2017) explored how the application of bamboo and rice straw
358 biochars with varying mesh sizes (0.25 and 1 mm) and at three different **levels** (0, 1, and 5% w/w)
359 affected the distribution of Cd in a contaminated sandy loam soil, using the BCR
360 (Bureau Communautaire de Référence) sequential extraction method. In contrast to the present
361 study, **they** reported that the biochars increased the concentration of the Cd-OM fraction, **and** this
362 was closely related to the increase in Cd immobilization. In another study, the application of sheep
363 manure biochar produced at 500 °C at the rate of 3% (w/w) to a Cd-contaminated calcareous soil
364 resulted in a significant increase **in Cd content in the OM fraction**, whereas the addition of other
365 biochar treatments (wheat straw, corn straw, rice husk, licorice root pulp) caused a significant
366 decrease in the concentration of Cd in the OM form when compared to the control soil (Boostani
367 et al., 2018b). In the study conducted by Boostani et al. (2018), the reduction **in Cd concentration**
368 **in the OM fraction** as affected by application of rice husk biochar is in line with our results,
369 however; the increase **in soil Cd in the OM form** with addition of sheep manure biochar is in
370 **contrast** with the result of the present study. **These observations indicate** in addition to the
371 characteristics of biochar and the level of its application (Lu et al., 2017), soil characteristics
372 (calcium carbonate percentage, soil texture, etc.) and the type of heavy metal can also have a
373 substantial role in the binding of PTEs to soil organic matter. By **application** the Si **levels** from S₀

374 to S₂, soil Ni content in the OM fraction was reduced by 16.8% (Table 4). To verify this finding,
375 Ma et al. (2021) reported that the application of Si to cultivated soils significantly reduced soil
376 organic matter content. They indicated that Si facilitates the decomposition and accessibility of
377 organic matter to plants. In this study, the interaction effects of biochars and Si levels showed that
378 the lowest Ni content in the OM fraction was due to the combined treatment of SM500+S₂ (7.12
379 mg Ni kg⁻¹ soil), which was equal to a 26.7% decrease compared to the control (CS₀) (9.72 mg Ni
380 kg⁻¹ soil) (Table 4).

381 All the biochar treatments caused a significant decrease in soil Ni concentration in the
382 MnOx fraction compared to the control, with the greatest reduction caused by the SM300 treatment
383 at 52.6% (Table 4). The lower temperature biochars were more effective than the higher
384 temperature biochars in decreasing the Ni content in the MnOx fraction (Table 4). In agreement
385 with the present study, Boostani et al. (2023c) observed that biochars produced from cow manure,
386 municipal solid waste and licorice root pulp at a lower pyrolysis temperature (300 °C) decreased
387 the soil Ni content in the MnOx fraction to a greater extent than those prepared at a higher
388 temperature (600 °C). Hydrophobicity of biochar is decreased with increasing pyrolysis
389 temperature (Kameyama et al., 2019). It is well known, at the same soil water content, the water
390 content of soil pores treated with biochars produced at lower pyrolysis temperatures is higher due
391 to lower absorption of water by the biochars. Therefore, in soils with high soil pore water content
392 and low oxygen conditions, the concentration of MnOx is decreased due to chemical reduction,
393 while concomitantly, the Mn concentration in the exchangeable and water-soluble are increased
394 (Sparrow and Uren, 2014). Furthermore, increasing the Si application levels from S₀ to S₂
395 significantly decreased the Ni content in the MnOx fraction by 17.6% (Table 4). Compared to the
396 control which had the highest concentration of Ni in the MnOx fraction (11.58 mg Ni kg⁻¹ soil),
397 the greatest interactive effect in the reduction of this fraction was related to the combined
398 SM300+S₂ (2.98 mg Ni kg⁻¹ soil) treatment by 3.8-fold (Table 4). The concentration of soil Ni
399 bound to the AFeOx and CFeOx fractions was significantly increased by application of Si levels
400 from S₀ to S₂ by 13.6% and 6.5%, respectively (Table 4). Belton et al. (2012) demonstrated that
401 exogenous silicon application resulted in the attachment of silicate to the surface of iron oxide in
402 the form of a polymer. Following the complexation of ferrosilicon, a significant number of
403 negatively charged functional groups, including silanol, were formed. These groups provided
404 numerous adsorption sites for PTEs, ultimately reducing their bioavailability (Belton et al., 2012).
405 In general, all the biochars caused a significant increase in soil Ni content in the form of CFeOx,
406 and there were no significant differences among the SM500, RH300 and RH500 treatments (Table
407 4). However, only the RH500 treatment increased the soil Ni concentration in the AFeOx fraction
408 compared to control (Table 4). Among all the biochars, only the SM300 resulted in a significant
409 increase in the soil Ni concentration in the Res fraction compared to the control (Table 4). The
410 application of Si levels also did not significantly affect on the Ni content in the Res fraction based
411 on the main effects (Table 4).

412 Mailakeba and Bk (2021) studied the addition of kunai grass biochar (0.75%) to a soil with
413 different Ni contamination levels (0, 56, 100, and 180 mg Ni kg⁻¹ soil). They found that the
414 application of the grass biochar increased soil Ni content in the Res fraction and reduced Ni in the
415 other fractions. In another study, Boostani et al. (2023c) demonstrated that the application of
416 biochars (cow manure, municipal compost and licorice root pulp each at 3%(w/w)) to a Ni-
417 contaminated soil increased soil Ni concentration in the fractions of OM and Res, and decreased
418 soil Ni content in the fractions of WsEx, Car, and Fe/Mn oxide. Whereas, Boostani et al. (2023b)

419 found that the application of manure and compost biochars (3% w/w) to Pb-contaminated soil did
420 not significantly affect the content of soil Pb in the Res fraction but did decrease the WsEx fraction.
421 Therefore, it seems that the effect of biochars on the changes of chemical fractions of PTEs in soil
422 depends on the raw materials and production conditions of the biochar, the soil application levels,
423 type of PTEs, the degree of soil contamination with PTEs, the selection of sequential extraction
424 procedure and the soil properties (Mailakeba and Bk, 2021; Boostani et al., 2023a, b; Boostani et
425 al., 2021).

426 In summary, the application of biochars in the present study resulted in the transfer of soil
427 Ni from more bioavailable and mobile fractions (WsEx, MnOx, OM) into other stable fractions
428 (AFeOx and CFeOx). These changes were particularly more evident in the WsEx fraction when
429 SM biochar was applied in conjunction with silicon, indicating that the simultaneous application
430 of these two substances is much more effective than applying them separately.

431 3.5 Shoot Ni concentration of *Zea mays L.* as affected by treatments

432 The main effects of biochars, Si application levels and their interactive effects were statistically
433 significant on the shoot Ni concentration of the corn. Application of Si levels from S₀ to S₂ resulted
434 in 32% decrease in shoot Ni concentration (Table 5). In addition, the shoot Ni concentration was
435 significantly decreased by application of all the biochar treatments compared to the control (with
436 no biochar addition) (Table 5). The interactive effects of treatments showed that the highest and
437 lowest shoot Ni concentration were due to the control (CS₀: without Si and biochar addition) (10.4
438 mg Ni kg⁻¹ DM) and SM500+S₂ (4.45 mg Ni kg⁻¹ DM) treatment, respectively (Table 5). The shoot
439 Ni concentration had a significant and positive correlation with the Ni-WsEx fraction ($r =$
440 $+0.62, P < 0.01$) while there were a significant and negative correlation between the soil pH ($r =$
441 $-0.60, P < 0.01$) and Ni-CFeOx fraction ($r = -0.50, P < 0.01$). This indicates that the
442 application of Si and biochar can reduce the shoot Ni concentration by increasing soil pH and, as
443 a result, reducing the amount of Ni in the fraction of WsEx and increasing the Ni content attached
444 to crystalline iron oxides. Boostani et al. (2019a) reported a significant reduction in the
445 concentration of Ni in spinach (*Spinacia oleracea L.*) shoots due to the application of rice husk
446 and licorice root pulp biochars (2.5% w/w) in a Ni-contaminated calcareous soil. Additionally,
447 they reported that the biochars produced at 350 °C were more effective at reducing crop Ni uptake
448 and promoting plant growth than the biochars produced at 550 °C. The most significant factors
449 that contribute to the uptake reduction of PTEs by plants in contaminated soils that have been
450 amended with biochars include adsorption of heavy metals by surface functional groups, increased
451 soil pH, reducing the mobility of PTEs by changing soil redox conditions, improved physical and
452 biological properties of the soil, changes in the activity levels of antioxidant enzymes, and a
453 decrease in the transfer of PTEs to the plant shoots (Zeng et al., 2018; Rizwan et al., 2016). Several
454 studies have investigated the effect of Si application on shoot Ni concentration and other heavy
455 metals in various plant species. Khaliq et al. (2016) observed a notable increase Ni concentration
456 and accumulation within the leaf, stem, and roots of cotton after Ni application. Whereas, Si
457 application was observed to induce a significant reduction in Ni concentrations across these
458 respective plant components. In another study, Maryam et al. (2024) concluded that addition of Si
459 caused an increase in the growth indices of maize through reducing the Pb concentration in shoots.
460 One possible explanation for the reduction of Ni concentration in shoots is that Si can compete

461 with Ni for uptake by plant roots. Silicon has a similar ionic radius to Ni, which means that it can
 462 occupy the same binding sites on root cell membranes and reduce the uptake of Ni. Additionally,
 463 Si can induce the expression of genes that are involved in Ni transport and homeostasis, which
 464 may contribute to the reduced **Ni concentration in shoots** (Hossain et al., 2012; Liang et al., 2005).

465

Table 5

Shoot Ni concentration (mg Ni kg⁻¹ DM) as affected by biochars and **Si application** levels.

	C	SM300	SM500	RH300	RH500	
S ₀	10.4 a	7.35 bc	9.85 a	7.55 bc	7.65 b	8.56 A
S ₁	7.65 b	6.90 bc	6.60 cd	7.05 bc	7.35 bc	7.11 B
S ₂	7.20 bc	5.05 ef	4.45 f	5.80 de	6.60 cd	5.82 C
Mean	8.41 A	6.43 C	6.96 BC	6.80 BC	7.20 B	

Notes: C, control; SM300, sheep manure biochar generated at 300 °C; SM500, sheep manure biochar generated at 500 °C; RH300, rice husk biochar produced at 300 °C; RH500, rice husk biochar produced at 500 °C; S₀, without Si application; S₁, addition of 250 mg Si kg⁻¹ soil; S₂, addition of 500 mg Si kg⁻¹ soil. Numbers followed by same letters in each section, are not significantly (P<0.05) different.

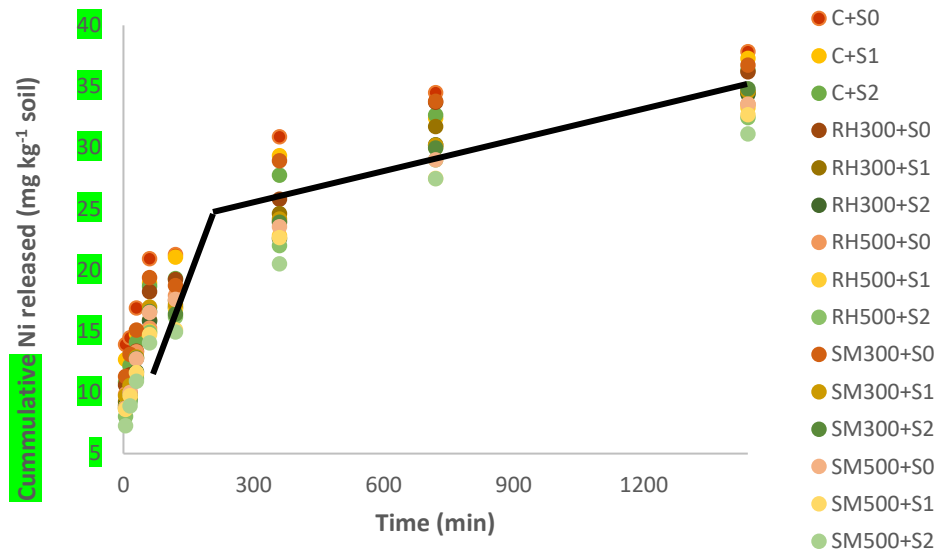
466

467 3.6 Soil Ni desorption as affected by **Si application levels** and biochars

468 The cumulative soil Ni desorption (extracted by DTPA) as a function of time are shown in
 469 **Figure 6**. The release of Ni from the soil initially proceeded at a much higher rate during the first
 470 hour, and then proceeded at a much slower rate during the next 24 hours, as illustrated by the trend-
 471 line in **Figure 6**. This two-stage process of releasing heavy metals from soil has also been reported
 472 by other researchers (Sajadi Tabar and Jalali, 2013; Boostani et al., 2023a). It is likely that the
 473 first stage of release is related to forms of Ni that are less strongly attached to soil particles,
 474 including WsEx and Car, while the second stage of desorption is likely from fractions of Ni with
 475 less bioavailability, such as FeOx and Res (Saffari et al., 2015). In general, the amount of soil Ni
 476 desorption was reduced by addition of biochars and Si levels (Fig. 6). In addition, the effects of
 477 biochars produced at **the higher pyrolysis temperature (500 °C)** on **reducing soil** Ni release was
 478 more than those generated at **the lower pyrolysis temperature (300 °C)**. The highest amount of soil
 479 Ni release was due to **the control (CS₀: without biochar and Si application)** (37.84 mg Ni kg⁻¹ soil)
 480 while the lowest was observed in the combined application of SM500 and S₂ (31.13 mg Ni kg⁻¹
 481 soil) treatment.

482

483



484

485 **Fig. 6.** Cumulative soil Ni desorption (extracted by DTPA) (mg kg^{-1}) as affected by different
 486 treatments. Notes: C, control; SM300, sheep manure biochar produced at 300°C ; SM500, sheep manure biochar
 487 produced at 500°C ; RH300, rice husk biochar produced at 300°C ; RH500, rice husk biochar produced at 500°C ; S₀,
 488 without Si addition; S₁, application of $250 \text{ mg Si kg}^{-1}$ soil; S₂, application of $500 \text{ mg Si kg}^{-1}$ soil.

489 3.7 Fitting of Ni release data to kinetic models

490 The soil Ni release data during 24 hours for all the biochar and Si treatments were evaluated
 491 by seven different kinetic models (Table 6). The effectiveness of the various kinetic models to
 492 describe the observed soil Ni desorption was analyzed by considering the coefficient of
 493 determination (R^2) and standard error of estimate (SEE), so that the highest value of the R^2 and the
 494 lowest value of the SEE were set as the criteria. As seen in Table 6, the order kinetic models did
 495 not adequately describe soil Ni release, and with the increase in the order of the kinetic model
 496 (from zero to third), the value of the R^2 decreased. This has also been found by other researchers
 497 for the release of heavy metals from soil (Boostani et al., 2019b; Ghasemi-Fasaee et al., 2006).
 498 Whereas, the non-order kinetic models, including power function, parabolic diffusion and simple
 499 Elovich, acceptably described the soil Ni release of the various treatments (Table 6). Among them,
 500 the power function model was the best according to the highest value of R^2 (0.98) and the lowest
 501 value of SEE (0.055). Boostani et al. (2018b) also reported that the power function was the best
 502 kinetic model to describe soil Cd desorption from a Cd-contaminated soil treated with biochars
 503 and zeolite.

504

505

506

507

508

509

Table 6

The range of coefficients of determination (R^2) and standard error of estimate (SEE) of applied kinetic models to all the soil treatments.

Kinetic models	R^2		SEE	
	Range	Mean	Range	Mean
Zero order	0.79-0.87	0.80	3.36-4.67	3.67
First order	0.69-0.75	0.75	0.22-0.29	0.25
Second order	0.53-0.61	0.52	0.011-0.026	0.0018
Third order	0.39-0.51	0.41	0.0013-0.0052	0.0030
Parabolic diffusion	0.94-0.98	0.96	1.26-2.44	1.85
Power function	0.97-0.99	0.98	0.054-0.057	0.055
Simple Elovich	0.92-0.97	0.95	2.04-2.78	2.50

510

511 3.8 Using the parameters of power function model to investigate the effect of treatments on soil
512 Ni desorption

513 As the power function model ($q = at^b$) described the soil Ni release data the best, its
514 parameters (a and b) were used to investigate the effect of biochar application and Si levels on the
515 release of Ni from the Ni-contaminated soil (Table 7). The main effects of biochars and Si levels
516 and their interactions on the 'a' and 'b' parameters were significant ($P < 0.01$). As Dang et al.
517 (1994) reported, in this kinetic model, a decrease in parameter 'a' and an increase in parameter 'b'
518 indicates a decrease in the rate of heavy metal desorption from the soil. The main effects of the
519 treatments showed that addition of all 4 biochars caused a significant decrease in the 'a' parameter
520 compared to the control while the 'b' parameter was significantly increased (Table 7). The same
521 trend was observed for all the Si treatment levels (Table 7). Therefore, it can be concluded that the
522 use of all the biochars and Si levels caused a decrease in the rate of Ni release from the Ni-
523 contaminated soil. Generally, there was a greater decrease in Ni desorption in biochar treatments
524 prepared at the higher temperature (Table 7). The interactive effects indicate that the most effective
525 combined treatment in reducing the rate of Ni release from the soil was SM500+S₂ which had the
526 lowest value of parameter 'a' (4.52) and the highest value of parameter 'b' (0.264) among the
527 treatments.

528 If it is differentiated from the power function equation ($q = at^b$) with respect to time (t)
529 ($dq/dt = ab t^{b-1}$), when $t = 1$ s = 0, the ratio of dq/dt becomes 'ab'. This parameter indicates the
530 amount of heavy metal desorption in the initial time (Dalal, 1985). The 'ab' parameter was affected
531 by the application of Si levels and biochars, so that this parameter was significantly decreased
532 compared to the control with addition of all the biochars (12.4%, 24.2%, 15.4% and 21.3% for the
533 SM300, SM500, RH300 and RH500, respectively) and Si application levels (13% from S₀ to S₂),
534 (Table 7). This finding also confirmed the effect of applied treatments in reducing the amount of
535 Ni release. The greatest reduction was observed in the combined treatment of SM500+S₂ by 33.5%
536 compared to the control (Table 7).

537

538

539

540

Table 7

The coefficients of the power function model as affected by biochars and Si application levels in a Ni-polluted calcareous soil after corn cultivation.

	C	SM300	SM500	RH300	RH500	
	a (mg Ni kg⁻¹ h⁻¹)^b					
S ₀	9.15 a	7.39 c	5.56 gh	6.49 e	5.95 f	6.91 A
S ₁	7.92 b	6.01 f	5.23 i	5.66 g	5.21 i	6.00 B
S ₂	6.90 d	5.39 hi	4.52 k	5.22 i	4.84 j	5.38 C
Mean	7.99 A	6.27 B	5.11 E	5.80 C	5.34 D	
	b (mg Ni kg⁻¹)⁻¹					
S ₀	0.196 i	0.222 g	0.247 d	0.238 e	0.237 e	0.228 C
S ₁	0.212 h	0.238 e	0.246 d	0.250 cd	0.254 bc	0.240 B
S ₂	0.230 f	0.254 bc	0.264 a	0.256 b	0.262 a	0.253 A
Mean	0.212 E	0.238 D	0.252 A	0.248 B	0.251 AB	
	ab					
S ₀	1.79 a	1.68 c	1.37 h	1.54 e	1.41 g	1.55 A
S ₁	1.69 b	1.43 f	1.29 k	1.41 fg	1.32 j	1.42 B
S ₂	1.59 d	1.37 h	1.19 m	1.34 i	1.27 l	1.35 C
Mean	1.69 A	1.48 B	1.28 E	1.43 C	1.33 D	

Notes: C, control; SM300, sheep manure biochar produced at 300 °C; SM500, sheep manure biochar produced at 500 °C; RH300, rice husk biochar produced at 300 °C; RH500, rice husk biochar produced at 500 °C; S₀, without Si addition; S₁, application of 250 mg Si kg⁻¹ soil; S₂, application of 500 mg Si kg⁻¹ soil.

541 * Numbers followed by same letters in each column and rows, in each section, are not significantly (P<0.05) different

542 The correlation between the parameters of the fitted power function model with soil Ni-
 543 chemical fractions, shoot Ni content and soil pH are shown in Table 8. The 'a' and 'ab' parameters
 544 had a positive correlation with the soil WsEx, OM and MnOx Ni fractions, while there was a
 545 negative correlation among the 'a' and 'ab' parameters the AFeOx and CFeOx Ni fractions. This
 546 trend was inverse for the 'b' parameter of the power function model. These correlations verified
 547 that the application of silicon and biochar to the Ni-contaminated calcareous soil led to a decrease
 548 in the rate and amount of Ni release from the soil by reducing the Ni concentration in chemical
 549 forms with higher bioavailability including WsEx, OM and MnOx. Furthermore, the 'a' and 'ab'
 550 parameters were negatively correlated with soil pH. Whereas there were positive correlations
 551 between these parameters and shoot Ni concentration (Table 8). These findings once again
 552 confirmed that the increase in soil pH due to the application of silicon and biochar can cause a
 553 decrease in the bioavailability of soil Ni and, as a result, a decrease in the concentration of Ni in
 554 aerial parts of the plant.

Table 8

The correlation coefficients (r) between the power function model parameters (a, b, ab) and soil Ni chemical fractions, shoot Ni concentration and soil pH.

	WsEx	Car	OM	MnOx	AFeOx	CFeOx	Res	Shoot Ni Concentration	Soil pH
a	0.63**	0.02 ^{ns}	0.70**	0.53**	-0.44**	-0.80**	0.27 ^{ns}	0.62**	-0.52**
b	-0.59**	0.03 ^{ns}	-0.68**	-0.54**	0.46**	0.83**	-0.28 ^{ns}	-0.63**	0.51**
ab	0.68**	0.04 ^{ns}	0.74**	0.46**	-0.46**	-0.80**	0.29 ^{ns}	0.06**	-0.51**

Notes: WsEx, water soluble and exchangeable fraction; OM, organic fraction; MnOx, bound to manganese oxides; AFeOx, bound to amorphous iron oxides; CFeOx, bound to crystalline iron oxides; Res, residual fraction.

** and ^{ns} indicate significance at the 0.01 probability level and non-significant, respectively.

555

556 4 Conclusions

557 The application of biochars and Si in the present study resulted in the transformation of Ni
558 in the soil from more bioavailable and mobile fractions (WsEx, MnOx, OM) to more stable forms
559 (AFeOx and CFeOx). These changes were particularly evident in the WsEx fraction when SM
560 biochars were applied in conjunction with silicon, indicating a strong synergistic effect related to
561 soil pH increase. Application of all biochars and Si reduced DPTA-extractable Ni release from the
562 soil, which was most strongly associated with the increase in CFeOx fraction. Application of all
563 biochars and Si decreased corn Ni uptake, with the combined SM500+S₂ being the most effective.
564 The decrease in corn uptake was correlated with the decrease in the WsEx-Ni fraction and increase
565 in CFeOx fraction. SM500 was likely the most effective biochar due to its higher alkalinity and
566 ash content, and lower acidic functional group content which enhances Ni sorption reactions with
567 Si. Future research is needed to better understand the mechanisms underlying the interaction
568 effects of Si and biochar application on the distribution of Ni chemical fractions in soil and to
569 optimize Si application strategies for sustainable Ni management in agricultural and natural
570 ecosystems. It is suggested that the interactive effects of Si and biochar on the soil Ni chemical
571 fractions and its release in aged Ni-contaminated soils should also be investigated and compared.

572 **Authors' Contributions** H.R.B. Conceptualization, Formal analysis, Methodology, Investigation,
573 Validation A.G.H. Writing - Review & Editing M.N. Project administration, Visualization E.B.
574 Review & Editing E.F. Laboratory analyses.

575 **Financial support.** No funding was received for conducting this study.

576 **Competing interests.** The contact author has declared that neither they nor their co-authors have
577 any competing interests.

578 **Data availability.** The data generated in this study are available from the corresponding authors
579 upon reasonable request.

580 **Disclaimer.** Publisher's note: Copernicus Publications remains neutral with regard to
581 jurisdictional claims in published maps and institutional affiliations.

582 **Acknowledgements:** This work was supported by College of Agriculture and Natural Resources of Darab,
583 Shiraz University, Darab, Iran.

584 References

- 585 Abdelhafez, A. A., Li, J., and Abbas, M. H.: Feasibility of biochar manufactured from organic wastes on
586 the stabilization of heavy metals in a metal smelter contaminated soil, *Chemosphere*, 117, 66-71,
587 2014.
- 588 Adrees, M., Ali, S., Rizwan, M., Zia-ur-Rehman, M., Ibrahim, M., Abbas, F., Farid, M., Qayyum, M. F.,
589 and Irshad, M. K.: Mechanisms of silicon-mediated alleviation of heavy metal toxicity in plants: a
590 review, *Ecotoxicology and Environmental Safety*, 119, 186-197, 2015.
- 591 Ahmad, M., Rajapaksha, A. U., Lim, J. E., Zhang, M., Bolan, N., Mohan, D., Vithanage, M., Lee, S. S.,
592 and Ok, Y. S.: Biochar as a sorbent for contaminant management in soil and water: a review,
593 *Chemosphere*, 99, 19-33, 2014.
- 594 Alam, M. S., Gorman-Lewis, D., Chen, N., Flynn, S. L., Ok, Y. S., Konhauser, K. O., and Alessi, D. S.:
595 Thermodynamic analysis of nickel (II) and zinc (II) adsorption to biochar, *Environmental science
596 & technology*, 52, 6246-6255, 2018.

597 Anand, A., Gautam, S., and Ram, L. C.: Feedstock and pyrolysis conditions affect suitability of biochar for
598 various sustainable energy and environmental applications, *Journal of Analytical and Applied*
599 *Pyrolysis*, 170, 105881, 2023.

600 Ankita Rao, K., Nair, V., Divyashri, G., Krishna Murthy, T., Dey, P., Samrat, K., Chandraprabha, M., and
601 Hari Krishna, R.: Role of Lignocellulosic Waste in Biochar Production for Adsorptive Removal of
602 Pollutants from Wastewater, in: *Advanced and Innovative Approaches of Environmental*
603 *Biotechnology in Industrial Wastewater Treatment*, Springer, 221-238, 2023.

604 Antoniadis, V., Levizou, E., Shaheen, S. M., Ok, Y. S., Sebastian, A., Baum, C., Prasad, M. N., Wenzel,
605 W. W., and Rinklebe, J.: Trace elements in the soil-plant interface: Phytoavailability, translocation,
606 and phytoremediation—A review, *Earth-Science Reviews*, 171, 621-645, 2017.

607 Bandara, T., Franks, A., Xu, J., Bolan, N., Wang, H., and Tang, C.: Chemical and biological immobilization
608 mechanisms of potentially toxic elements in biochar-amended soils, *Critical Reviews in*
609 *Environmental Science and Technology*, 50, 903-978, 2020.

610 Belton, D. J., Deschaume, O., and Perry, C. C.: An overview of the fundamentals of the chemistry of silica
611 with relevance to biosilicification and technological advances, *The FEBS journal*, 279, 1710-1720,
612 2012.

613 Bharti, K. P., Pradhan, A. K., Singh, M., Beura, K., Behera, S. K., and Paul, S. C.: Effect of mycorrhizal
614 co-Inoculation with selected rhizobacteria on soil zinc dynamics, *International Journal of Current*
615 *Microbiology and Applied Sciences*, 7, 1961-1970, 2018.

616 Bhat, J. A., Shivaraj, S., Singh, P., Navadagi, D. B., Tripathi, D. K., Dash, P. K., Solanke, A. U., Sonah,
617 H., and Deshmukh, R.: Role of silicon in mitigation of heavy metal stresses in crop plants, *Plants*,
618 8, 71, 2019.

619 Boostani, H., Hardie, A., Najafi-Ghiri, M., and Khalili, D.: Investigation of cadmium immobilization in a
620 contaminated calcareous soil as influenced by biochars and natural zeolite application, *International*
621 *journal of environmental science and technology*, 15, 2433-2446, 2018a.

622 Boostani, H., Hardie, A., Najafi-Ghiri, M., and Khalili, D.: Investigation of cadmium immobilization in a
623 contaminated calcareous soil as influenced by biochars and natural zeolite application, *International*
624 *Journal of Environmental Science and Technology*, 15, 2433-2446, 2018b.

625 Boostani, H. R., Hardie, A. G., and Najafi-Ghiri, M.: Chemical fractions, mobility and release kinetics of
626 Cadmium in a light-textured calcareous soil as affected by crop residue biochars and Cd-
627 contamination levels, *Chemistry and Ecology*, 1-14, 2023a.

628 Boostani, H. R., HARDIE, A. G., and NAJAFI-GHIRI, M.: Lead stabilization in a polluted calcareous soil
629 using cost-effective biochar and zeolite amendments after spinach cultivation, *Pedosphere*, 33, 321-
630 330, 2023b.

631 Boostani, H. R., Najafi-Ghiri, M., and Mirsoleimani, A.: The effect of biochars application on reducing the
632 toxic effects of nickel and growth indices of spinach (*Spinacia oleracea* L.) in a calcareous soil,
633 *Environmental Science and Pollution Research*, 26, 1751-1760, 2019a.

634 Boostani, H. R., Hardie, A. G., Najafi-Ghiri, M., and Khalili, D.: The effect of soil moisture regime and
635 biochar application on lead (Pb) stabilization in a contaminated soil, *Ecotoxicology and*
636 *Environmental Safety*, 208, 111626, 2021.

637 Boostani, H. R., Hardie, A. G., Najafi-Ghiri, M., and Zare, M.: Chemical speciation and release kinetics of
638 Ni in a Ni-contaminated calcareous soil as affected by organic waste biochars and soil moisture
639 regime, *Environmental Geochemistry and Health*, 45, 199-213, 2023c.

640 Boostani, H. R., Najafi-Ghiri, M., Amin, H., and Mirsoleimani, A.: Zinc desorption kinetics from some
641 calcareous soils of orange (*Citrus sinensis* L.) orchards, southern Iran, *Soil science and plant*
642 *nutrition*, 65, 20-27, 2019b.

643 Chatterjee, R., Sajjadi, B., Chen, W.-Y., Mattern, D. L., Hammer, N., Raman, V., and Dorris, A.: Effect of
644 pyrolysis temperature on physicochemical properties and acoustic-based amination of biochar for
645 efficient CO₂ adsorption, *Frontiers in Energy Research*, 8, 85, 2020.

646 Claoston, N., Samsuri, A., Ahmad Husni, M., and Mohd Amran, M.: Effects of pyrolysis temperature on
647 the physicochemical properties of empty fruit bunch and rice husk biochars, *Waste Management*
648 & *Research*, 32, 331-339, 2014.

649 Dalal, R.: Comparative prediction of yield response and phosphorus uptake from soil using anion-and
650 cation-anion-exchange resins, *Soil Science*, 139, 227-231, 1985.

651 Dang, Y., Dalal, R., Edwards, D., and Tiller, K.: Kinetics of zinc desorption from Vertisols, *Soil Science*
652 *Society of America Journal*, 58, 1392-1399, 1994.

653 Deng, Y., Huang, S., Laird, D. A., Wang, X., and Meng, Z.: Adsorption behaviour and mechanisms of
654 cadmium and nickel on rice straw biochars in single-and binary-metal systems, *Chemosphere*, 218,
655 308-318, 2019.

656 Derakhshan Nejad, Z., Jung, M. C., and Kim, K.-H.: Remediation of soils contaminated with heavy metals
657 with an emphasis on immobilization technology, *Environmental geochemistry and health*, 40, 927-
658 953, 2018.

659 Dey, D., Sarangi, D., and Mondal, P.: Biochar: Porous Carbon Material, Its Role to Maintain Sustainable
660 Environment, in: *Handbook of Porous Carbon Materials*, Springer, 595-621, 2023.

661 El-Naggar, A., Rajapaksha, A. U., Shaheen, S. M., Rinklebe, J., and Ok, Y. S.: Potential of biochar to
662 immobilize nickel in contaminated soils, in: *Nickel in Soils and Plants*, CRC Press, 293-318, 2018.

663 El-Naggar, A., Chang, S. X., Cai, Y., Lee, Y. H., Wang, J., Wang, S.-L., Ryu, C., Rinklebe, J., and Ok, Y.
664 S.: Mechanistic insights into the (im) mobilization of arsenic, cadmium, lead, and zinc in a multi-
665 contaminated soil treated with different biochars, *Environment International*, 156, 106638, 2021.

666 Gao, W., He, W., Zhang, J., Chen, Y., Zhang, Z., Yang, Y., and He, Z.: Effects of biochar-based materials
667 on nickel adsorption and bioavailability in soil, *Scientific Reports*, 13, 5880, 2023.

668 Gee, G. W. and Bauder, J. W.: Particle-size analysis, *Methods of soil analysis: Part 1 Physical and*
669 *mineralogical methods*, 5, 383-411, 1986.

670 Ghasemi-Fasaei, R., Maftoun, M., Ronaghi, A., Karimian, N., Yasrebi, J., Assad, M., and Ippolito, J.:
671 Kinetics of copper desorption from highly calcareous soils, *Communications in Soil Science and*
672 *Plant Analysis*, 37, 797-809, 2006.

673 Ghiri, M. N., Abtahi, A., Owliaie, H., Hashemi, S. S., and Koohkan, H.: Factors affecting potassium pools
674 distribution in calcareous soils of southern Iran, *Arid land research and management*, 25, 313-327,
675 2011.

676 Hossain, M. A., Piyatida, P., da Silva, J. A. T., and Fujita, M.: Molecular mechanism of heavy metal toxicity
677 and tolerance in plants: central role of glutathione in detoxification of reactive oxygen species and
678 methylglyoxal and in heavy metal chelation, *Journal of botany*, 2012, 2012.

679 Ippolito, J., Berry, C., Strawn, D., Novak, J., Levine, J., and Harley, A.: Biochars reduce mine land soil
680 bioavailable metals, *Journal of environmental quality*, 46, 411-419, 2017.

681 Kamali, S., Ronaghi, A., and Karimian, N.: Soil zinc transformations as affected by applied zinc and organic
682 materials, *Communications in soil science and plant analysis*, 42, 1038-1049, 2011.

683 Kameyama, K., Miyamoto, T., and Iwata, Y.: The preliminary study of water-retention related properties
684 of biochar produced from various feedstock at different pyrolysis temperatures, *Materials*, 12,
685 1732, 2019.

686 Kandpal, G., Srivastava, P., and Ram, B.: Kinetics of desorption of heavy metals from polluted soils:
687 Influence of soil type and metal source, *Water, Air, and Soil Pollution*, 161, 353-363, 2005.

688 Keiluweit, M., Nico, P. S., Johnson, M. G., and Kleber, M.: Dynamic molecular structure of plant biomass-
689 derived black carbon (biochar), *Environmental science & technology*, 44, 1247-1253, 2010.

690 Khaliq, A., Ali, S., Hameed, A., Farooq, M. A., Farid, M., Shakoor, M. B., Mahmood, K., Ishaque, W., and
691 Rizwan, M.: Silicon alleviates nickel toxicity in cotton seedlings through enhancing growth,
692 photosynthesis, and suppressing Ni uptake and oxidative stress, *Archives of Agronomy and Soil*
693 *Science*, 62, 633-647, 2016.

694 Li, X.: Technical solutions for the safe utilization of heavy metal-contaminated farmland in China: a critical
695 review, *Land Degradation & Development*, 30, 1773-1784, 2019.

696 Liang, Y., Wong, J., and Wei, L.: Silicon-mediated enhancement of cadmium tolerance in maize (*Zea mays*
697 L.) grown in cadmium contaminated soil, *Chemosphere*, 58, 475-483, 2005.

698 Lindsay, W. L. and Norvell, W.: Development of a DTPA soil test for zinc, iron, manganese, and copper,
699 *Soil science society of America journal*, 42, 421-428, 1978.

700 Liu, L., Guo, X., Wang, S., Li, L., Zeng, Y., and Liu, G.: Effects of wood vinegar on properties and
701 mechanism of heavy metal competitive adsorption on secondary fermentation based composts,
702 *Ecotoxicology and environmental safety*, 150, 270-279, 2018.

703 Loeppert, R. H. and Suarez, D. L.: Carbonate and gypsum, *Methods of soil analysis: Part 3 chemical*
704 *methods*, 5, 437-474, 1996.

705 Lu, K., Yang, X., Gielen, G., Bolan, N., Ok, Y. S., Niazi, N. K., Xu, S., Yuan, G., Chen, X., and Zhang,
706 X.: Effect of bamboo and rice straw biochars on the mobility and redistribution of heavy metals
707 (Cd, Cu, Pb and Zn) in contaminated soil, *Journal of environmental management*, 186, 285-292,
708 2017.

709 Ma, C., Ci, K., Zhu, J., Sun, Z., Liu, Z., Li, X., Zhu, Y., Tang, C., Wang, P., and Liu, Z.: Impacts of
710 exogenous mineral silicon on cadmium migration and transformation in the soil-rice system and on
711 soil health, *Science of the Total Environment*, 759, 143501, 2021.

712 Mailakeba, C. D. and BK, R. R.: Biochar application alters soil Ni fractions and phytotoxicity of Ni to
713 pakchoi (*Brassica rapa L. ssp. chinensis L.*) plants, *Environmental Technology & Innovation*, 23,
714 101751, 2021.

715 Maruyama, M., Sawada, K. P., Tanaka, Y., Okada, A., Momma, K., Nakamura, M., Mori, R., Furukawa,
716 Y., Sugiura, Y., and Tajiri, R.: Quantitative analysis of calcium oxalate monohydrate and dihydrate
717 for elucidating the formation mechanism of calcium oxalate kidney stones, *Plos one*, 18, e0282743,
718 2023.

719 Maryam, H., Abbasi, G. H., Waseem, M., Ahmed, T., and Rizwan, M.: Preparation and characterization of
720 green silicon nanoparticles and their effects on growth and lead (Pb) accumulation in maize (*Zea*
721 *mays L.*), *Environmental Pollution*, 123691, 2024.

722 Myszk, B., Schüßler, M., Hurle, K., Demmert, B., Detsch, R., Boccaccini, A. R., and Wolf, S. E.: Phase-
723 specific bioactivity and altered Ostwald ripening pathways of calcium carbonate polymorphs in
724 simulated body fluid, *RSC advances*, 9, 18232-18244, 2019.

725 Nasrabadi, M., Omid, M. H., and Mazdeh, A. M.: Experimental Study of Flow Turbulence Effect on
726 Cadmium Desorption Kinetics from Riverbed Sands, *Environmental Processes*, 9, 10, 2022.

727 Nelson, D. W. and Sommers, L. E.: Total carbon, organic carbon, and organic matter, *Methods of soil*
728 *analysis: Part 3 Chemical methods*, 5, 961-1010, 1996.

729 Okolo, C. C., Gebresamuel, G., Zenebe, A., Haile, M., Orji, J. E., Okebalama, C. B., Eze, C. E., Eze, E.,
730 and Eze, P. N.: Soil organic carbon, total nitrogen stocks and CO₂ emissions in top-and subsoils
731 with contrasting management regimes in semi-arid environments, *Scientific Reports*, 13, 1117,
732 2023.

733 Poznanović Spahić, M. M., Sakan, S. M., Glavaš-Trbić, B. M., Tančić, P. I., Škrivanj, S. B., Kovačević, J.
734 R., and Manojlović, D. D.: Natural and anthropogenic sources of chromium, nickel and cobalt in
735 soils impacted by agricultural and industrial activity (Vojvodina, Serbia), *Journal of Environmental*
736 *Science and Health, Part A*, 54, 219-230, 2019.

737 Rhoades, J.: Salinity: Electrical conductivity and total dissolved solids, *Methods of soil analysis: Part 3*
738 *Chemical methods*, 5, 417-435, 1996.

739 Rizwan, M., Ali, S., Qayyum, M. F., Ibrahim, M., Zia-ur-Rehman, M., Abbas, T., and Ok, Y. S.:
740 Mechanisms of biochar-mediated alleviation of toxicity of trace elements in plants: a critical
741 review, *Environmental Science and Pollution Research*, 23, 2230-2248, 2016.

742 Sachdeva, S., Kumar, R., Sahoo, P. K., and Nadda, A. K.: Recent advances in biochar amendments for
743 immobilization of heavy metals in an agricultural ecosystem: A systematic review, *Environmental*
744 *Pollution*, 319, 120937, 2023.

745 Saffari, M., Karimian, N., Ronaghi, A., Yasrebi, J., and Ghasemi-Fasaei, R.: Stabilization of nickel in a
746 contaminated calcareous soil amended with low-cost amendments, *Journal of soil science and plant*
747 *nutrition*, 15, 896-913, 2015.

748 Sajadi Tabar, S. and Jalali, M.: Kinetics of Cd release from some contaminated calcareous soils, *Natural*
749 *resources research*, 22, 37-44, 2013.

750 Shahbazi, K., Fathi-Gerdelidani, A., and Marzi, M.: Investigation of the status of heavy metals in soils of
751 Iran: A comprehensive and critical review of reported studies, *Iranian Journal of Soil and Water*
752 *Research*, 53, 1163-1212, 10.22059/ijswr.2022.341586.669245, 2022.

753 Shahbazi, K., Marzi, M., and Rezaei, H.: Heavy metal concentration in the agricultural soils under the
754 different climatic regions: a case study of Iran, *Environmental earth sciences*, 79, 324, 2020.

755 Shahzad, B., Tanveer, M., Rehman, A., Cheema, S. A., Fahad, S., Rehman, S., and Sharma, A.: Nickel;
756 whether toxic or essential for plants and environment-A review, *Plant Physiology and*
757 *Biochemistry*, 132, 641-651, 2018.

758 Shen, B., Wang, X., Zhang, Y., Zhang, M., Wang, K., Xie, P., and Ji, H.: The optimum pH and Eh for
759 simultaneously minimizing bioavailable cadmium and arsenic contents in soils under the organic
760 fertilizer application, *Science of the Total Environment*, 711, 135229, 2020.

761 Singh, J., Karwasra, S., and Singh, M.: Distribution and forms of copper, iron, manganese, and zinc in
762 calcareous soils of India, *Soil Science*, 146, 359-366, 1988.

763 Sparks, D. L., Singh, B., and Siebecker, M. G.: *Environmental soil chemistry*, Elsevier2022.

764 Sparrow, L. and Uren, N.: Manganese oxidation and reduction in soils: effects of temperature, water
765 potential, pH and their interactions, *Soil Research*, 52, 483-494, 2014.

766 Sumner, M. E. and Miller, W. P.: Cation exchange capacity and exchange coefficients, *Methods of soil*
767 *analysis: Part 3 Chemical methods*, 5, 1201-1229, 1996.

768 Sun, L., Zhang, G., Li, X., Zhang, X., Hang, W., Tang, M., and Gao, Y.: Effects of biochar on the
769 transformation of cadmium fractions in alkaline soil, *Heliyon*, e12949, 2023.

770 Sun, Y., Gao, B., Yao, Y., Fang, J., Zhang, M., Zhou, Y., Chen, H., and Yang, L.: Effects of feedstock type,
771 production method, and pyrolysis temperature on biochar and hydrochar properties, *Chemical*
772 *engineering journal*, 240, 574-578, 2014.

773 Tomczyk, A., Sokołowska, Z., and Boguta, P.: Biochar physicochemical properties: pyrolysis temperature
774 and feedstock kind effects, *Reviews in Environmental Science and Bio/Technology*, 19, 191-215,
775 2020.

776 Uchimiya, M., Lima, I. M., Thomas Klasson, K., Chang, S., Wartelle, L. H., and Rodgers, J. E.:
777 Immobilization of heavy metal ions (CuII, CdII, NiII, and PbII) by broiler litter-derived biochars
778 in water and soil, *Journal of agricultural and food chemistry*, 58, 5538-5544, 2010.

779 Vickers, N. J.: Animal communication: when i'm calling you, will you answer too?, *Current biology*, 27,
780 R713-R715, 2017.

781 Xiao, Z., Peng, M., Mei, Y., Tan, L., and Liang, Y.: Effect of organosilicone and mineral silicon fertilizers
782 on chemical forms of cadmium and lead in soil and their accumulation in rice, *Environmental*
783 *Pollution*, 283, 117107, 2021.

784 Yan, G.-c., Nikolic, M., YE, M.-j., Xiao, Z.-x., and LIANG, Y.-c.: Silicon acquisition and accumulation in
785 plant and its significance for agriculture, *Journal of Integrative Agriculture*, 17, 2138-2150, 2018.

786 Yuan, J.-H., Xu, R.-K., and Zhang, H.: The forms of alkalis in the biochar produced from crop residues at
787 different temperatures, *Bioresource technology*, 102, 3488-3497, 2011.

788 Zemnukhova, L. A., Panasenko, A. E., Artem'yanov, A. P., and Tsoy, E. A.: Dependence of porosity of
789 amorphous silicon dioxide prepared from rice straw on plant variety, *BioResources*, 10, 3713-3723,
790 2015.

791 Zeng, X., Xiao, Z., Zhang, G., Wang, A., Li, Z., Liu, Y., Wang, H., Zeng, Q., Liang, Y., and Zou, D.:
792 Speciation and bioavailability of heavy metals in pyrolytic biochar of swine and goat manures,
793 *Journal of Analytical and Applied Pyrolysis*, 132, 82-93, 2018.

794 Zhao, S.-X., Ta, N., and Wang, X.-D.: Effect of temperature on the structural and physicochemical
795 properties of biochar with apple tree branches as feedstock material, *Energies*, 10, 1293, 2017.

796 Zhu, Q., Wu, J., Wang, L., Yang, G., and Zhang, X.: Effect of biochar on heavy metal speciation of paddy
797 soil, *Water, Air, & Soil Pollution*, 226, 1-10, 2015.
798